Proceedings of the 2001 IEEE
International Conference on Robotics & Automation
Seoul, Korea - May 21-26, 2001

Sensor Based Planning for Rod Shaped Robots in Three Dimensions: Piece-wise Retracts of $\mathbb{R}^3 \times S^2$

Ji Yeong Lee, Howie Choset and Alfred A. Rizzi, *Carnegie Mellon University*

Abstract

We describe a new roadmap, termed the rod-HGVG, for motion planning of a rod-shaped robot operating in a three-dimensional volume. This roadmap is defined in terms of work space distance enabling us to prescribe an incremental construction procedure. This allows the rod to explore its configuration space, $\mathbb{R}^3 \times S^2$, without ever explicitly constructing the configuration space. In fact, the rod robot need not know the work space ahead of time. We term the rod-HGVG a piecewise retract because it comprises many retracts. Homotopy theory asserts that there cannot be in general a one-dimensional retract of non-contractable five-dimensional space. Instead, we define an exact cellular decomposition on $\mathbb{R}^3 \times S^2$ and a retract in each cell. Next, we "connect" the retracts of each cell forming a piece-wise *retract of the rod's configuration space.*

1 Introduction

This work considers the sensor based planning of a rod robot in three dimensions. Although planning for rod-shaped robots is geometrically similar to planning for blimp robots, ultimately motion planning for highly articulated robots motivates this research and the motion planning of a rod robot is the first step toward this goal. In this paper, we will define a roadmap for a rod robot in three dimensions. This roadmap is the *rod hierarchical generalized Voronoi graph* (rod-HGVG). Recall from Canny's roadmap work [1] that for each connected component of free space, a roadmap has the following properties : (i) accessibility, (ii) departability, and (iii) connectivity. This means that if there exists a path between two configurations, we can determine a path by first finding a path to the roadmap from the start configuration, then following the roadmap, and then finding another path from the roadmap to the destination. If a planner can incrementally construct a roadmap, then it has in essence explored the configuration space.

Canny's original roadmap work required *a priori* information about the robot's configuration space, and hence was difficult to implement. The probabilistic community [5], [9] has successfully demonstrated the capabilities of probabilistic roadmaps for highly articulated robots; their approach does not construct the configuration space, but requires knowledge of the work space prior to the planning event. Rimon [8] first suggested a method for constructing roadmap using"critical point" sensors, but did not provide details on these sensors. Choset and Burdick developed a method to construct the Voronoi Graph in the plane and in three dimensions without requiring *a priori* workspace or configuration space information [2]. Later, Choset extended this result to a rod-shaped robot operating in the plane [3]. This method enabled a rod robot to map its configuration space without any prior information of its workspace (and configuration space). Loosely speaking, the rod-HGVG in $\mathbb{R}^3$ can be viewed as a combination of two prior roadmaps : (i) the point-HGVG, which is a roadmap for the point robot operating in a three-dimensional space, and (ii) the planar Rod-HGVG, which is a roadmap for rod robot operating in the plane. The rod-HGVG will be defined in terms of the distance information that sensors can easily provide, and it can be generated in an unknown environment.

1.1 The Generalized Voronoi Graph in $\mathbb{R}^2$ and $\mathbb{R}^3$

Ó'Dúnlaing and Yap [7] first applied the *generalized Voronoi Diagram* (GVD) to path planning of a disk-shaped robot. This result requires full knowledge of the environment to construct the roadmap and is restricted to the plane. Choset and Burdick extended this result beyond the plane by defining the *generalized Voronoi graph* (GVG) [2] which is a roadmap for a point robot operating either in the plane or in three dimensions. The GVG can be constructed using line of sight sensor data because it is defined in terms of the distance function,

$$d_i(r) = \min_{c \in C_i} \|r - c\|,$$

where $r \in FS$, $FS \subset R^2$ is the free space and C_i is an obstacle. A *point-two-equidistant face* is defined as

$$\begin{aligned} F_{ij} \;=\; & \{r \in FS : d_i(r) = d_j(r), \\ & \nabla d_i(r) \neq \nabla d_j(r) \text{ and} \\ & d_i(r) \leq d_h(r)\ \forall h \neq i,j\} \end{aligned} \tag{1}$$

In planar case, F_{ij} is one-dimensional and the GVG is the union of F_{ij}'s, i.e., for an environment with n obstacles, the GVG is $\cup_{i=1}^{n-1} \cup_{j=i+1}^{n} F_{ij}$.

In $\mathbb{R}^3$, the *point-three-equidistant face* defines the GVG. That is,

$$\begin{aligned} F_{ijk} \;=\; & \{r \in FS : d_i(r) = d_j(r) = d_k(r) \\ & \nabla d_i(r) \neq \nabla d_j(r), \nabla d_i(r) \neq \nabla d_k(r), \\ & \nabla d_j(r) \neq \nabla d_k(r), \text{and} \\ & d_i(r) \leq d_h(r) \forall h \neq i,j,k\} \end{aligned} \tag{2}$$

A three-equidistant face can also be defined as the intersection of two-equidistant faces, i.e., $F_{ijk} = F_{ij} \cap F_{jk} \cap F_{ik}$. However, we assume that the intersections are transversal [2] which is a different way of saying that the obstacles all lie in general position. The GVG is the union of the F_{ijk}'s, is one-dimensional, and not necessarily connected in $\mathbb{R}^3$. To connect the GVG, we will need to define additional structures, resulting in the *hierarchical generalized Voronoi graph* (HGVG) [2]. To distinguish the GVG from the rod-GVG, in later sections, we call this GVG defined in this section as point-GVG.

1.2 The Rod-HGVG in SE(2)

O'Dúnlaing, Sharir and Yap [6] extended their disk-result to rod-shaped robots, but this result also requires full knowledge of the environment and is restricted to the plane. Cox and Yap developed an "on-line" strategy for rod path-planning [4], but this result does not provide a roadmap of the rod robot's free space. In this section, we describe the *rod-hierarchical generalized Voronoi graph* (rod-HGVG) in the plane. This structure provides the groundwork for the rod-robot roadmap in three dimensions.

The rod in the plane has three degrees-of-freedom, and we represent a rod configuration as $q = (x, y, \theta)^T$. As with the point-GVG, we first define the distance function. Let q be a rod configuration, and $R(q)$ be the set of all points that the rod occupies at configuration q. Then, the distance between the obstacle C_i and the rod at q is defined as

$$D_i(q) = \min_{r \in R(q), c \in C_i} \|r - c\|.$$

The rod-GVG is the set of configurations equidistant to three obstacles. More formally, we first define the *rod-two-equidistant face* as follows

$$\begin{aligned} CF_{ij} &= \{q \in SE(2) : D_i(q) = D_j(q) \leq D_h(q) \forall h \neq i, j \\ &\quad \text{and } \nabla D_i(q) \neq \nabla D_j(q)\}. \end{aligned}$$

Then, the *rod-three-equidistance face* is defined as

$$CF_{ijk} = CF_{ij} \cap CF_{jk} \cap CF_{ik}.$$

In the planar case, we term the rod-three-equidistant faces as *rod-GVG edges*. The rod-GVG is simply the union of the rod-GVG edges, i.e., the set of rod configurations that are three-way equidistant. The rod-four-equidistance faces, which can be defined similarly, are termed *rod-meet points*, which correspond to configurations of the rod where rod-GVG edges intersect and terminate.

The rod-GVG edges are not necessarily connected, even in the planar case. To produce a connected structure we introduce another type of edge, called *R-edges*.

Fig. 1. The Rod GVG-edge and R-edge in $\mathbb{R}^2$.

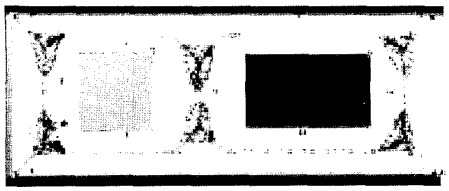

Fig. 2. The Rod-HGVG in $\mathbb{R}^2$.

An R-edge is the set of rod configurations defined as,

$$\begin{aligned} \mathcal{R}_{ij} &= \{q \in cl(RF_{ij})) : r \in F_{ij} \text{ and} \\ &\quad (i)\ 0 \leq d_i(r) \leq d_i(r_1)\ \forall r_1 \in R(q) \text{ and} \\ &\quad (ii)\ d_i(r) \leq D_h(q)\ \forall h \neq i, j\}, \end{aligned}$$

where RF_{ij} is the collection of lines tangent to F_{ij} (which can be viewed as a "tangent bundle" of F_{ij}) [3]. Roughly speaking, R-edges connect the disconnected rod-GVG edges using point-GVG edges. The rod-HGVG then comprises Rod-GVG edges and R-edges. Figures 1 and 2 show an example of the rod-HGVG in $\mathbb{R}^2$.

We demonstrate connectivity of the rod [3] by defining a *piece-wise* retraction $H : \mathcal{FS} \times [0, 1] \rightarrow CF_{ijk}$. This H function also describes how the rod accesses the rod-GVG. The rod accesses the planar rod-GVG (and hence the rod-HGVG) via two gradient ascent operations: while maintaining a fixed orientation, the rod moves away from its closest obstacle and then while maintaining double equidistance and a fixed orientation, the rod moves away from the two closest obstacles until it reaches triple equidistance. Note that $\theta(q) = \theta(H(q, t))$ for all $t \in [0, 1]$, i.e., the rod arrives to the rod-GVG with a fixed orientation.

In order to "make" H continuous, we divide the configuration space $R^2 \times S^1$ into junction regions J_{ijk} where each junction region J_{ijk} is the pre-image of CF_{ijk} under H. This essentially guarantees that CF_{ijk} is a retract of J_{ijk}. Finally, note that if the rod is "small" enough, CF_{ijk} has one connected component and is diffeomorphic to S^1.

For each connected component of a junction region J_{ijk}, there is a connected component of CF_{ijk}. If motion planning should occur only in one junction region, then planning is trivial because CF_{ijk} is a retract of J_{ijk}. If the union of the CF_{ijk}'s formed a connected set, then planning is trivial again. In general, the CF_{ijk}'s will not form a connected set in $\mathbb{R}^2 \times S^1$, so we use the point-GVG to connect the CF_{ijk}'s of the junction regions.

The connections between junction regions are the rod configurations tangent to the point GVG, i.e., the R-edges.

Essentially, we are forming an exact cellular decomposition of $R^2 \times S^1$ where the junction regions are the cells. Planning in a cell is achieved with the rod-GVG edges, CF_{ijk}, and planning between the cells is achieved with the R-edges. We take an analogous approach to defining the rod-HGVG for the rod in three dimensions.

2 Rod-HGVG in $\mathbb{R}^3 \times S^2$, based on the point-GVG

In this section, we define the rod-HGVG. Since the rod's configuration space $\mathbb{R}^3 \times S^2$ has five dimensions, it is natural to first define a five-way equidistant structure which we term *rod-GVG edges*. Just like the planar rod-GVG, the three-dimensional rod-GVG (henceforth called the rod-GVG), is not necessarily connected. Just like the planar case, we decompose $\mathbb{R}^3 \times S^2$ into cells, also called *junction regions*, and "connect" them with *1-tangent edges*, structures that are analogous to R-edges. However, the rod-GVG edges by themselves are not retracts of the junction regions. Instead, the set of configurations equidistant to *four* obstacles forms a retract of a junction region. This four-way equidistant structure has two dimensions, and thus this structure, with the 1-tangent edges and rod-GVG edges do not form a roadmap. Therefore, we define an additional structures called *2-tangent edges*, which are four-way equidistant with an additional constraint. The rod-HGVG comprises rod-GVG edges, 1-tangent edges, and 2-tangent edges. This section formally defines these structures and the next two sections establish that the rod-HGVG is a roadmap.

2.1 Rod-GVG Edges

The rod-GVG is the set of configurations that are equidistant to five obstacles. The definition of the distance function in $\mathbb{R}^3 \times S^2$ is identical to that in SE(2), i.e., $D_i(q) = \min_{r \in R(q), c \in C_i} \|r - c\|$, but the rod configuration q is parametrized by $q = (x, y, z, \theta, \varphi)^T$. Note that $\theta(q)$ and $\varphi(q)$ define the orientation of the rod. The rod gradient is derived in Appendix A. With distance and its gradient defined, we can define rod-equidistant faces, continuing from where we left off in the planar case. The *rod-four-equidistant face* is

$$CF_{ijkl} = CF_{ijk} \cap CF_{ikl} \cap CF_{jkl}.$$

Then the *rod-five-equidistant face*, which is a *rod-GVG edge* in the three-dimensional case, is defined as

$$CF_{ijklm} = CF_{ijkl} \cap CF_{iklm} \cap CF_{jklm}.$$

A *rod-meet point* is then CF_{ijklmn}, the zero-dimensional set of rod configurations that are six-way equidistant.

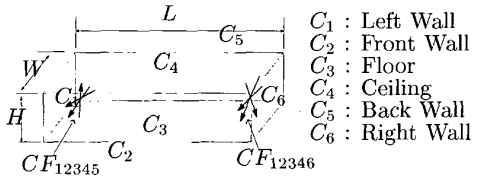

Fig. 3. Here, there are two set of rod configurations that are five-way equidistant. The configurations in CF_{12345} are equidistant to C_1, C_2, C_3, C_4 and C_5, and the configurations in CF_{12346} are equidistant to C_1, C_2, C_3, C_4 and C_6. Note that they are not connected to each other.

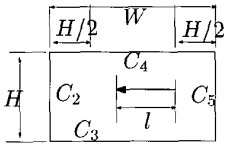

Fig. 4. Side view of Fig. 3 with $L > W, L > H$, but here, the length of the rod is smaller than $W - H$, thus, the rod cannot be four-way equidistant to C_2, C_3, C_4 and C_5. Therefore, five-way equidistant configurations do not exist either.

The rod-GVG edges can be generated by tracing the roots of the following function

$$G(q) = \begin{pmatrix} (D_i - D_j)(q) \\ (D_i - D_k)(q) \\ (D_i - D_l)(q) \\ (D_i - D_m)(q) \end{pmatrix}.$$

In the rod configuration space $\mathbb{R}^3 \times S^2$, the collection of rod-GVG edges is not necessarily connected, and in many environments, it may not even exist at all. Figure 3 shows a rectangular environment, where $L > W > H$ and CF_{12345} and CF_{12346} are the rod-GVG edges. If L is substantially larger than the length of the rod, there cannot be any six-way equidistant configurations, so these two component cannot be connected. Now, if W is also substantially larger than the length of the rod, the five-way equidistant configuration cannot exist (Figure 4).

2.2 1-tangent edges

The rod-GVG defined above will not necessarily be connected. Just like the rod-GVG in the planar case, we use the point-GVG to define additional structures that connect disconnected rod-GVG edge. These structures are similar to the R-edges where the rod is "tangent" to the point-GVG edge. More specifically, when C_i, C_j and C_k define a point-GVG edge F_{ijk}, we presume that

- The rod is "tangent" to F_{ijk} at r.
- At r, $d_n(r) < d_n(r_o)$ for all other points r_o on the rod, and for all three closest obstacles $C_n, n = i, j, k$, i.e, the point r is the closest to all three ob-

stacles.

The second condition asserts that $r_i = r_j = r_k$, where r_i, r_j and r_k are the closest points on the rod to each obstacles [3].

Instead of calling this an R-edge. we term this structure the *1-tangent edge* because it is tangent to a one-dimensional structure from the point-GVG. We can use the same technique as in the planar case to construct R-edge to construct this 1-tangent edge. The rod finishes the tracing a 1-tangent edge when it (i) reaches a four-way equidistant configuration, (ii) reaches an obstacle boundary, or (iii) detects the cycle. A cycle in the GVG is a disconnected edge diffeomorphic to S^1. Note that we consider only environments where the point-GVG is connected, and thus the condition (iii) will not occur.

2.3 2-tangent edges

Consider two 1-tangent edges that terminate at configurations equidistant to the same four obstacles. These two end point configurations cannot coincide with each other because we assume that the point-equidistant faces transversally intersect each other. In other words, two 1-tangent edges cannot intersect each other. The set of four-way equidistant configurations is two-dimensional and thus we need an additional constraint to define a one-dimensional structure that connects the two 1-tangent edges.

Consider the rod-four-equidistant face CF_{ijkl} with 1-tangent edge R_{ijk} and R_{ijl} each terminating at configurations in CF_{ijkl} (boundedness of the workspace assures this can happen). For R_{ijk}, the rod lies in the tangent space associated with F_{ijk}; restated, the rod simultaneously lies in the tangent spaces of F_{ij}, F_{ik}, and F_{jk}. Likewise, for R_{ijl}, the rod lies in tangent spaces F_{ij}, F_{il}, and F_{jl}. Note that in both cases, the rod lies in the tangent space associated with F_{ij}. Therefore, as our additional constraint, to travel from R_{ijk} to R_{ijl} along CF_{ijkl}, the rod must remain in the tangent space of F_{ij}. The edge formed on CF_{ijkl} with the additional constraint of staying in the tangent space of F_{ij} is termed a *2-tangent-edge* because the rod lies in a two-dimensional tangent space (as opposed to a one-dimensional tangent space with the 1-tangent edge). Note that for CF_{ijkl}, there are four 1-tangent edges that terminate on the set, and there can be six different 1-tangent edges on it.

As an example, the Figure 5 shows the case where F_{ij} is a plane. Here, the rod is "tangent" to $F_{ceiling,floor}$ when the rod is moving from q_2 to q_3, and "tangent" to $F_{front,floor}$ when moving from q_1 to q_2. Generally, when the rod is tracing four equidistant configuration from a configuration tangent to F_{ijk} to a configuration tangent to F_{jkl}, it must be in tangent space of F_{kl}.

Now we describe the tangent condition for 2-tangent edge $R_{ij/kl}$ more specifically, and demonstrate it is one-

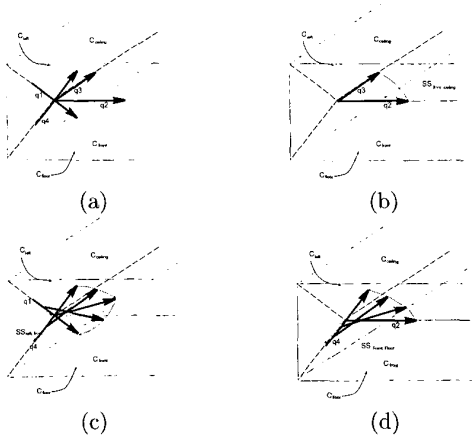

Fig. 5. In figure (a), q_1, q_2, q_3 and q_4 represent four-way equidistant configurations. Also they are terminal configurations. of different 1-tangent edges. Figures (b), (c) and (d) shows 2-tangent edges that connect some pairs of 1-tangent edges.

dimensional. First we need to define some additional structures. We define the set of rod configurations q in CF_{ij} that satisfy the conditions (i) q is tangent to F_{ij} (ii) $r_i = r_j$, where r_i and r_j are the points on the rod closest to each obstacles C_i and C_j as RC_{ij}, i.e.,

$$\begin{aligned} RC_{ij} \quad = \quad & \{q \in cl(RF_{ij})) : r \in F_{ij} \text{ and} \\ & (i)\ 0 \le d_i(r) \le d_i(r_1)\ \forall r_1 \in R(q) \text{ and} \\ & (ii)\ d_i(r) \le D_h(q)\ \forall h \neq i,j\},. \end{aligned}$$

where, RF_{ij} is the set of planes tangent to F_{ij} (which is analogous to a tangent bundle of F_{ij}). We form the 2-tangent edge $R_{ij/kl}$ by intersecting RC_{ij} and CF_{ijkl}, i.e., $R_{ij/ik} = RC_{ij} \cap CF_{ijkl}$.

Note that $RC_{ij} \cap CF_{ijkl} = RC_{ij} \cap CF_{jkl}$ As shown in Appendix B, RC_{ij} is three dimensional. Since CF_{ikl} and RC_{ij} are each three dimensional, $R_{ij/kl}$ is generally one-dimensional by the pre-image theorem.

The $R_{ij/kl}$ can be constructed by tracing the roots of

$$G(q) = \begin{pmatrix} (D_i - D_j)(q) \\ (D_i - D_k)(q) \\ (D_i - D_l)(q) \\ (r_i - r_j)(q) \end{pmatrix}$$

Here, the first three elements ensures the four-way equidistance. The fourth element forces the two closest points on the rod to C_i and C_j to be the same and thus specifies the orientation of the rod. Since sensors can easily provide distance information and determine the closest points on the rod to the closest obstacles, the 2-tangent edge can be readily constructed without *a prior* information.

3 Accessibility

The rod accesses the rod-GVG (and hence the rod-HGVG) via four gradient ascent operations: the first three use a fixed orientation gradient $\tilde{\nabla} D_i(x)$ that directs the rod to increase distance to an object C_i while maintaining its orientation; the last gradient ascent operation uses the full gradient $\nabla D_i(x)$ which is derived in the Appendix. The first three gradient ascent operations implicitly define a function $H^3 : \mathcal{FS} \times [0,1] \rightarrow CF_{ijkl}$ that is analogous to the H mapping which enables a rod to access the planar rod-GVG. First, while maintaining a fixed orientation, the rod moves away from its closest obstacle (i.e., $\dot{c}(t) = \tilde{\nabla} D_i(c(t))$), then while maintaining double equidistance and a fixed orientation, the rod moves away from the two closest obstacles until it reaches triple equidistance (i.e., $\dot{c}(t) = \pi_{T_{c(t)}CF_{ij}} \tilde{\nabla} D_i(c(t))$, where $\pi_{T_{c(t)}CF_{ij}}$ is the projection operator), and then while maintaining triple equidistance and a fixed orientation, the rod moves away from the three closest obstacles until it reaches four-way equidistance (i.e., $\dot{c}(t) = \pi_{T_{c(t)}CF_{ijk}} \tilde{\nabla} D_i(c(t))$).

Finally, we define another mapping $HJ : CF_{ijkl} \rightarrow R_{ij/kl} \bigcup CF_{ijklm}$ that moves the rod away from the four closest obstacles, using the full gradient,

$$\dot{c}(t) = \pi_{T_{c(t)}CF_{ijkl}} \nabla D_i(c(t))$$

This step terminates at either of the following : (i) five-way equidistance, i.e., a rod-GVG edge, or (ii) a 2-tangent edge (proof appears in Appendix C). Once the rod has accessed the rod-HGVG, it can then begin incrementally constructing the rod-HGVG using the previously defined numerical techniques. If the rod-HGVG is connected, then numerically constructing it ensures complete exploration of a connected component of the rod's configuration space.

4 Connectivity

We will demonstrate that if the point-GVG is connected, then there exists a path between two rod configurations $q_1, q_2 \in \mathbb{R}^3 \times S^2$ if and only if there exists a path between two rod configurations q_1^*, q_2^* on the rod-HGVG in $\mathbb{R}^3 \times S^2$. Note that q_1^*, q_2^* are the "projected" configurations onto the rod-HGVG from q_1, q_2 via a mapping $HJ \circ H^3 : \mathbb{R}^3 \times S^2 \times [0,1] \rightarrow$ rod-HGVG.

The H^3 mapping is analogous to a retraction and is defined in a similar fashion as H in the planar case. In $\mathbb{R}^3 \times S^2$, we will take a similar approach as the planar case to "make" H^3 continuous; here, we define junction regions that are J_{ijkl} and the connections among them are the 1-tangent edges R_{ijk}, the set of rod configurations tangent to the point-GVG edge CF_{ijk}.

A junction region J_{ijkl} is the pre-image of CF_{ijkl} under $H^3 : \mathbb{R}^3 \times S^2 \times [0,1] \rightarrow CF_{ijkl}$. Again, H^3 is implicitly defined by a sequence of three fixed-orientation gradient ascent operations. Note that $\theta(q) = \theta(H^3(q,1))$ and $\phi(q) = \phi(H^3(q,1))$ and using a similar approach as in [3], H^3 can be shown to be continuous in each junction region J_{ijkl}. Therefore, CF_{ijkl} is a two-dimensional retract of J_{ijkl}. In fact, if the rod is "small" enough, CF_{ijkl} is diffeomorphic to a two-sphere, S^2. At this point, we can infer that if the point-GVG is connected in $\mathbb{R}^3$, then there exists a path between q_1 and q_2 in $\mathbb{R}^3 \times S^2$ if and only if there exists a path between $H^3(q_1,1)$ and $H^3(q_2,1)$ in the union of 1-tangent edges R_{ijk} and rod-four-equidistant faces CF_{ijkl}.

We have not defined a roadmap yet because CF_{ijkl} has two dimensions, not one. To define a one-dimensional structure on CF_{ijkl}, we define another mapping $HJ : CF_{ijkl} \rightarrow R_{ij/kl} \bigcup CF_{ijklm}$. This function is also implicitly defined via a gradient ascent operation. From Section 3, we showed that once the rod achieves four-way equidistance, continued gradient ascent (full gradient ascent) brings the rod either to a two-tangent edge $R_{ij/kl}$ or a rod-GVG edge CF_{ijklm}.

If the rod is "small" enough, then this last gradient ascent operation brings the rod only to a two-tangent edge. If the rod is "large" enough, the two-spheres CF_{ijkl} and CF_{ijkm} intersect and form an edge CF_{ijklm} and gradient ascent could bring the rod to a five-way equidistant configuration (but can also bring the rod to a 2-tangent edge). If the rod is even larger (or obstacles are appropriately shaped), a rod-meet-point occurs when three two-sphere intersect.

For the sake of discussion, lets assume the rod is "small" enough so no two-sphere intersect with each other. In other words, lets assume there are no rod-GVG edges and rod-meet-points on the rod-four-equidistant faces. If HJ were continuous on a rod-four-equidistant face, then the two-tangent edges would form a retract of the rod-four-equidistant faces and we are done.

Alas, this is not the case. Instead, we define another cellular decomposition on CF_{ijkl} where each cell is denoted $J_{ij/kl}$ and is defined by the pre-image of $R_{ij/kl}$ under the HJ mapping. For each cell $J_{ij/kl}$, HJ is continuous and therefore $R_{ij/kl}$ is a one-dimensional retract of $J_{ij/kl}$.

The remaining challenge is to establish that the two-tangent edges "link up" properly. This is easily shown because each end point of the 1-tangent edges coincides with the end point of three different 2-tangent edges. Consider the 1-tangent edge R_{ijk}; it has two types of end points: a boundary configuration and a four-way equidistant configuration (i.e., equidistant to C_l in addition to C_i, C_j and C_k.) Consider the end point that is four-way equidistant. By definition of the 1-tangent edge, its end point is tangent to the point-GVG edge F_{ijk}, which means that the end point is also tangent to

Fig. 6. Rod-HGVG in a rectangular box.

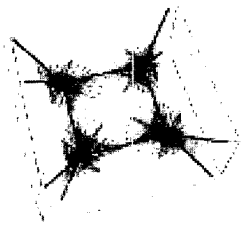

Fig. 7. Rod-HGVG in an square box. In this example the rod-HGVG does not exist, and junction regions are connected by 1-tangent edges

the point-two-equidistant faces F_{ij}, F_{jk} and F_{ik}. Therefore, this end point also belongs to the 2-tangent edges $R_{ij/kl}$, $R_{jk/il}$ and $R_{ik/jl}$. This shows that three of the six 2-tangent edges connect. By repeating this argument for the other combination of 1-tangent edges and 2-tangent edges, one can easily see how all of the 2-tangent edges link up.

5 Simulation Result

We performed a computer simulation using the algorithm described in this paper. Figures 6 and 7 shows the complete rod-HGVG in simple environments. For more simulation results, see `http://voronoi.sbp.ri.cmu.edu`.

6 Conclusion

This paper introduces a roadmap called *rod hierarchical generalized Voronoi graph* for a rod-shaped robot operating in a three-dimensional space. The rod-HGVG is defined in terms of workspace distance information, which sensors can easily provide. Using work space distance information, we can prescribe a sensor-based incremental method to achieve motion planning without constructing the configuration space. This is important for sensor based planning because we cannot construct configuration space without knowing the workspace first. Moreover, even when we have configuration space representation, it is still difficult to measure the distance in configuration space than in workspace. The rod-HGVG has three components : (i) rod-GVG edges, which are five-way equidistant, (ii) 2-tangent edges, which are four-way equidistant and (iii) 1-tangent edges, which are three-way equidistant.

The first contribution of this paper is the piece-wise retract: we defined an exact cellular decomposition of the rod's configuration space where in each cell, called a junction region, we defined a retract that makes motion planning in the junction region trivial. We then use the point-GVG to connect the retracts of each junction region, which is the second contribution of this paper. We were able to use connectivity of a structure defined in the robot's workspace to infer connectivity properties of the robot's configuration space. In other words, when connectivity of the point-GVG represents the connectivity of the works space, then connectivity of the rod-HGVG represents the connectivity of the rod's configuration space.

In general the point-GVG is not connected in $\mathbb{R}^3$, so future work will use the point-HGVG to connect the junction regions. We started with the point-GVG only to achieve a tractable subgoal. We also defined a piecewise retract on CF_{ijkl} to guarantee connectivity of the rod-HGVG. This relied on HJ being continuous, which due to space limitations, was not detailed in this paper; a rigorous proof should be demonstrated.

Ideally, we would like to demonstrate this on a robot blimp. This work is a step towards the ultimate goal of sensor based planning for an articulated multi-body robot. The next step is to consider two rod robots, and then an n-rod robot.

References

[1] J.F. Canny. *The Complexity of Robot Motion Planning.* MIT Press, Cambridge, MA, 1988.

[2] H. Choset and J. Burdick. Sensor based motion planning: The hierarchical generalized voronoi graph. *International Journal of Robotics Research*, 19(2):96–125, February 2000.

[3] H. Choset and J.W.Burdick. Sensor Based Planning for a Planar Rod Robot. In *Proc. IEEE Int. Conf. on Robotics and Automation*, 1996.

[4] J. Cox and C.K. Yap. On-line Motion Planning: Case of a Planar Rod. In *Annals of Mathematics and Artificial Intelligence*, volume 3, pages 1–20, 1991.

[5] Jean-Claude Latombe, Lydia E. Kavraki, Peter Svestka, and Mark Overmars. Probablistic roadmaps for path planning in high dimensional configuration spaces. *IEEE Transactions on Robotics and Automation*, 12(4):566–580, 1996.

[6] C. Ó'Dúnlaing, M. Sharir, and C.K. Yap. Generalized Voronoi Diagrams for Moving a Ladder. I: Topological Analysis. *Communications on Pure and Applied Mathematics*, 39:423–483, 1986.

[7] C. Ó'Dúnlaing and C.K. Yap. A "Retraction" Method for Planning the Motion of a Disc. *Algorithmica*, 6:104–111, 1985.

[8] E. Rimon and J.F. Canny. Construction of C-space Roadmaps Using Local Sensory Data — What Should the Sensors Look For? In *Proc. IEEE Int. Conf. on Robotics and Automation*, pages 117–124, San Diego, CA, 1994.

[9] Steven A. Wilmarth, Nancy M. Amato, and Peter F. Stiller. Motion planning for a rigid body using random networks on

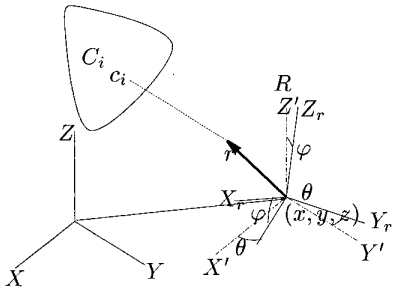

Fig. 8. World and Body coordinate system for the Rod

the medial axis of the free space. In *Proceedings of the 15th Annual ACM Symposium on Computational Geometry*, pages 173–180, June 1999.

Appendix

A Rod Gradient

Here, we derive the rod distance gradient. In Fig. 8, X, Y and Z denote the world coordinate frame, and X_r, Y_r and Z_r denote the body fixed coordinate frame on R (the rod). Let $(x, y, z)^T$ be the origin of the body fixed coordinate frame, and θ, φ be the orientation of the body fixed coordinate frame with respect to world coordinate frame. Let c be the closest point on the obstacle C_i to the robot and r be the closest point to C_i on the robot. Finally let $(a, b, c)^T$ be the coordinate of r in body fixed coordinate frame. Then the world coordinate of r is

$$r = \begin{bmatrix} x + a\cos\theta\cos\varphi - b\sin\theta + c\cos\theta\sin\varphi \\ y + a\sin\theta\cos\varphi + b\cos\theta + c\sin\theta\sin\varphi \\ z - a\sin\varphi + c\cos\varphi \end{bmatrix}$$

Then, following similar steps to the two dimensional case [3], the first three components of the distance gradient are

$$[\frac{\partial D}{\partial x}, \frac{\partial D}{\partial y}, \frac{\partial D}{\partial z}] = \frac{1}{D_i(q)}[(r_x - c_x), (r_y - c_y), (r_z - c_z)]$$

The remaining two rotational components are

$$\frac{\partial D}{\partial \theta} = \frac{1}{D_i(q)} \left\langle \begin{bmatrix} c_x - r_x \\ c_y - r_y \\ c_z - r_z \end{bmatrix}, \begin{bmatrix} aS\theta C\varphi + bC\theta + cS\theta S\varphi \\ -aC\theta C\varphi + bS\theta - cC\theta S\varphi \\ 0 \end{bmatrix} \right\rangle$$

$$\frac{\partial D}{\partial \varphi} = \frac{1}{D_i(q)} \left\langle \begin{bmatrix} c_x - r_x \\ c_y - r_y \\ c_z - r_z \end{bmatrix}, \begin{bmatrix} aC\theta S\varphi - cC\theta C\varphi \\ aS\theta S\varphi + cS\theta C\varphi \\ aC\varphi + cC\varphi \end{bmatrix} \right\rangle$$

B Dimension of RC_{ij}

In this section, we show that RC_{ij} is three-dimensional. Note that for any rod configuration $q \in CF_{ij}$, $R(q) \cap F_{ij}$ is not empty, and without loss of generality, we assume that $R(q) \cap F_{ij}$ is zero dimensional, i.e., a single point. For rod configurations in RC_{ij}, $r_i = r_j = R(q) \cap F_{ij}$. We call that point the "contact point" and simply denote it as r. We define the *constant distance curve* $cv_{ij}(\Omega)$ on F_{ij} as the set of all points on F_{ij} that have distance Ω to C_i, i.e.

$$cv_{ij}(\Omega) = \{x \in F_{ij} : d_i(x) = \Omega\}.$$

Now we consider the contact condition and dimensionality of RC_{ij}, in two separate cases, depending on the contact point r for each rod configurations: (I) $d_i(r)$ is at local mininum of the distance on F_{ij} to C_i on F_{ij}. (II) otherwise.

LEMMA B.1 *For rod configurations in CF_{ij} that are tangent to F_{ij} and $r_i = r_j$, such that $d_i(r_i)$ is not a local minimum of the distance (i.e., Case II above), (a) the contact point r must be either an end point P or Q, or (b) the rod must be in the tangent space of $cv_{ij}(d_i(r))$ and the contact point can be an interior point of the rod. Also, when the rod satisfies case (II) above, the rod has one degree of freedom in this set when the contact point is fixed.*

Proof: Note that, in a neighborhood about the origin of $T_r cv_{ij}$, $T_r cv_{ij}(d_i(r))$ separates the $T_r F_{ij}$ into two regions, such that all the points in one region have distance less than $d_i(r)$ to C_i, and the points in the other region have greater distance. for case (a), by hypothesis, the rod lies in a line that transversally intersects $T_r cv_{ij}(d_i(r))$. So, if $r \neq P, Q$, the rod itself intersects $T_r cv_{ij}(d_i(r))$ in its interior. So loosely speaking, P and Q are on opposite sides of $T_r cv_{ij}(d_i(r))$.

Let's define a set $L_i(\Omega)$, such that

$$L_i(\Omega) = \{x \in \mathbb{R}^3 : d_i(x) = \Omega\}.$$

This set is a two dimensional manifold in $\mathbb{R}^3$. Note that $cv_{ij}(d_i(r))$ can be seen as the intersection of $L_i(d_i(r))$ and F_{ij}. Because the rod intersects $T_r cv_{ij}(d_i(r))$ at r and r is on $L_i(d_i(r))$, the rod must "poke" into $L_i(d_i(r))$. This contradicts the condition that the point r is the closest point on the rod to each obstacles. So the rod cannot intersect the $cv_{ij}(d_i(r))$ in its interior, i.e., the intersection must occur at a rod's end point P or Q, when the intersection in transversal.

If the rod "touches" cv_{ij} at P or Q (case (a)), the rod cannot translate, but can rotate around the contact point as long as it "stays" on the tangent space $T_r F_{ij}$. When the rod is "tangent" to cv_{ij} (case (b)), the rod cannot change its rotation, but translate along its length. Therefore, when the contact point is fixed on F_{ij}, the rod has one degree of freedom in each cases. Because F_{ij} is two dimensional, the rod has three degrees of freedom in RC_{ij}. Figure 9 describe this case. ■

LEMMA B.2 *For case (i) above, the contact point can be one of the interior points on the rod, and the rod has two degrees of freedom at each configuration in this set.*

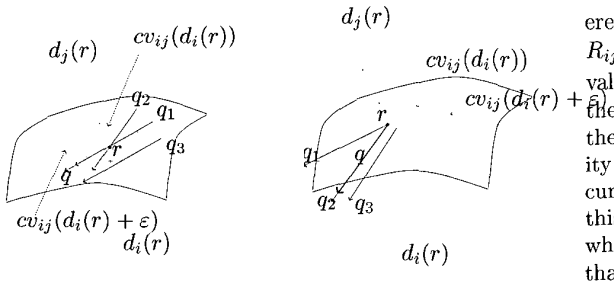

Fig. 9. Figure(a) :The rod configuration q touches F_{ij} at r, which is not a local minimum, and the rod is also tangent to $cv_{ij}(d_i(r))$. The three degrees of freedom that rod has are: (i) it can slide along its length (q_1) (ii) it can move "on" $cv_{ij}(d_i(r))$, maintaining the tangent condition to it (q_2). and (iii) it can slide normal to its length and become tangent to $cv_{ij}(d_i(r)+\varepsilon)$ (q_3). Figure(b) :The rod configuration q touches F_{ij} at r, which is not a local minimum, and the rod touches $cv_{ij}(d_i(r))$ at Q. The three degrees of freedom that the rod has are: (i) it can rotate around Q on the tangent plane (q_1). (ii) it can move "on" $cv_{ij}(d_i(r))$ (q_3) and (iii) it can move on F_{ij}, to $cv_{ij}(d_i(r))+\varepsilon(q_3)$.

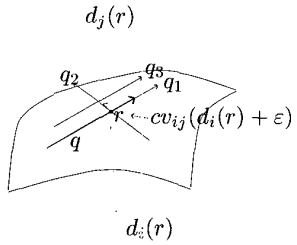

Fig. 10. When the rod touches F_{ij} at local minimum r, the rod has three degrees of freedom in the set R_{ij}. q is the original configuration. Then it can slide along its length (q_1), it can rotate around r (q_2) and it can slide without rotation so that it becomes tangent to $cv_{ij}(d_i(r)+\varepsilon)$ (q_3).

Proof: Let's call the set of rod configurations that satisfy case (i) as R^1_{ij}. This is a subset of RC_{ij}. In this case, $L_i(d_i(r)) \cap F_{ij}$ is a single point , which means that these two surfaces contact at a single point r, and share a common tangent plane at that point. Then, while the rod satisfies this condition, the rod is free to move on that plane, as long as $r \in R(q)$. That means that the rod has two degrees of freedom in this set R^1_{ij}, i.e. this set has two degrees of freedom. Because this set R^1_{ij} is subset of R_{ij}, the rod configuration in the set R^1_{ij} has at least two degrees of freedom in the set R_{ij}. Now, let's consider whether there are any additional degrees of freedom for the rod in the set R_{ij}. Because the dimension of the set R^1_{ij} is two, if the rod has any additional degrees of freedom in R_{ij}, the movements in those directions will move the rod outside of the set R^1_{ij}, but not outside of the R_{ij}. And of course those movements must be independent from the movement we already considered. Recall that when the rod configuration belongs to $R_{ij} - R^1_{ij}$, the rod must be "tangent" to $cv_{ij}(d)$ for some value of d. Now if the rod moves outside the set R^1_{ij}, the distances to C_i and C_j increase. Let's denote that the new distance as $d_i(r)+\varepsilon$. Then, from the continuity of the distance function the $cv_{ij}(d_i(r)+\varepsilon)$ is a closed curve around the point r. The rod must be "tangent" to this curve, and there are only two point on that curve where the tangent is parallel to the rod. That means that the rod has (only) one more additional degree of freedom (which moves the rod outside of the R^1_{ij}, thus makes the rod lost contact at r, but still the rod stays in R_{ij}) at the given configuration in R^1_{ij}. Thus the rod has three degrees of freedom in this case. (Figure 10) ■

C Accessibility Proof

In this section, we demonstrate that a rod starting at a four-way equidistant configuration will access either (i) a rod-GVG edge or (ii) a 2-tangent edge via full gradient ascent of distance to the four closest obstacles. Proving case (i) is trivial. Now, we prove case (ii), i.e., the gradient ascent will eventually direct the rod onto the $R_{ij/kl}$ when there are no five-way equidistant configurations. Figure 11(a) shows a rod configuration which intersects SS_{lk} nontraversally. Consider the plane formed by the rod vector PQ and the vector $r_k c_k$. Then let the global coordinate frame be located such that (i) the origin is located on P, (ii) the X and Y axes are on the plane formed by PQ and $r_k c_k$. Then the Z axis of the global coordinate frame is perpendicular to that frame. In this frame, the rod configuration is at $(0,0,0,0,0)$ and the body fixed coordinate of the r is $(a,0,0)$ with some positive value a. Note that in this coordinate system, the θ component of the gradient rotates the rod "in" the plane, ane the φ component of the gradient rotates the rod out of the plane. We interested in the θ component, which for the obstacle C_k is $\frac{\partial D_k}{\partial \theta} = \frac{1}{D_i(q)} \left\langle [c^x_k - r^x_k, c^y_k - r^y_k, 0]^T, [a_k \sin\theta, -a_k \cos\theta, 0]^T \right\rangle$. Then, the two vectors $(c^k_k - r^x_k, c^y_k - r^x_k, 0)^T$ and $(a_k \sin\theta, -a_k \cos\theta, 0)^T$ are parallel. So $\partial D_k / \partial\theta$ has positive value, and that means that the angle between the tangent plane on SS_{kl} and the rod increases as a result of gradient ascent. Now do the same analysis with $r_l c_l$; the vector $r_l c_l$ is in the "opposite" direction of $(a_k \sin\theta, -a_k \cos\theta, 0)^T$ and the coordinate value of a_l is larger because r_l is on the other side of SS_{kl}. This means that the gradient for C_l has a negative component of $\frac{\partial D_l}{\partial \theta}$ on plane defined by PQ and $r_l c_l$, with larger value than $\frac{\partial D_k}{\partial \theta}$, i.e., $\frac{\partial D_l}{\partial \theta} > \frac{\partial D_k}{\partial \theta}$. This decreases the angle between the tangent plane and the rod. Thus, the angle between the tangent plane and the rod will decrease during the gradient ascent, forcing the rod to become tangent.

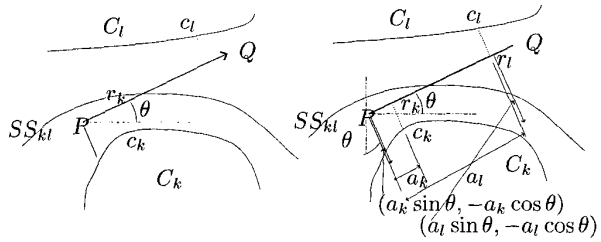

Fig. 11. The rod is two-way equidistant to obstacles C_k and C_l. The rod intersects SS_kl transvesally. In second figure, the rod is shown on the plane defined by PQ and r_kc_k. Also in this figure r_lc_l is on the same plane, but in general it will be on different plane.